MedCrave
Step into the World of Research

Pharmacy & Pharmacology International Journal

Research Article

Open Access

CrossMark

Design of experiment based optimization of an *in vitro* direct contact triculture blood brain barrier model for permeability screening

Abstract

The *in vivo* restrictive properties of the blood brain barrier (BBB) largely arise from astrocyte and pericyte synergistic cell signaling interactions that underlie the brain microvessel endothelial cells (BMEC). *In vivo* relevant direct contact between astrocytes, pericytes, and BMECS, to our knowledge, has not been established in conventional Transwell® based *in vitro* screening models of the BBB. We hypothesize that a design of experiments (DOE) optimized direct contact layered triculture model will offer more *in vivo* relevance for screening in comparison to indirect models. Plating conditions including the seeding density of all three cell types, matrix protein, and culture time were assessed utilizing a DOE approach. A second set of DOE methods assessed the influence of medium additives on barrier properties. The optimized model was further assessed for p-glycoprotein function using a substrate and inhibitor along with a set of BBB paracellular and transcellular markers at varying permeation rates. The optimization revealed that length of culture post endothelial cell plating correlated highest with paracellular tightness. In addition, seeding density of the endothelial cell layer influenced paracellular tightness at earlier times of culture, and its impact decreased as culture is extended. At optimal conditions, the model revealed P-gp function along with the ability to differentiate between BBB positive and negative permeants. We have demonstrated that the implementation of DOE based optimization for biologically based systems is an expedited method to establish multi-component *in vitro* cell models. The direct contact BBB triculture model reveals that the physiologically relevant layering of the three cell types is a practical method of culture to establish a screening model compared to indirect plating methods that incorporate physical barriers between cell types. Additionally, the ability of the model to differentiate between BBB positive and negative permeants suggests that this model may be an enhanced screening tool for potential neuroactive compounds.

Keywords: blood brain barrier, permeability, design of experiments, optimization, astrocytes, pericytes, brain microvessel endothelium, triculture, direct cell-cell contact

Volume 9 Issue 4 - 2021

Kelsey E Lubin, Gregory T Knipp
Department of Industrial and Physical Pharmacy, College of Pharmacy, Purdue University, USA

Correspondence: Gregory T Knipp, Department of Industrial and Physical Pharmacy, College of Pharmacy, Purdue University, 575 Stadium Mall Drive, West Lafayette, Indiana 47907, USA, Tel 765-494-3765, Fax 765-494-6545, Email gknipp@purdue.edu

Received: July 19, 2021 | **Published:** July 28, 2021

Abbreviations: ABC, ATP binding cassette; BBB, blood brain barrier; BCRP, breast cancer resistant protein; BMEC, brain microvessel endothelial cell; DMEM/F-12, Dulbecco's Modified Eagle Medium/Nutrient Mixture F-12; DMSO, dimethylsulfoxide; DOE, design of experiments; ECGS, endothelial cell growth supplement; ECM, extracellular matrix; FBS, fetal bovine serum; FITC, Fluorescein isothiocyanate; GLUT-1, glucose transporter 1; HBSS, Hank's balanced salt solution; HBEC-5i, human brain endothelial cell; hCMEC/D3, human cerebral microvessel endothelial cell; HEPES, 2-[4-(2-hydroxyethyl)piperazin-1-yl]ethanesulfonic acid; ICAM-1, intercellular adhesion molecule 1; NVU, neurovascular unit; OFAT, one factor at a time; Papp, apparent permeability; PBS, phosphate buffered saline; PDGF-B, platelet-derived growth factor B; Peff, effective permeability; PECAM-1, platelet endothelial cell adhesion molecule 1; P-gp, p-glycoprotein; PLL, poly-L-lysine; R123, rhodamine 123; TEER, transendothelial electrical resistance; TGF-β, transforming growth factor-β; TNF-α, tumor necrosis factor-α; VCAM-1, vascular adhesion molecule 1; ZO-1, zonula occluden 1

Introduction

There is a continuing need for screening models that will facilitate the development of therapeutic agents aimed at mitigating brain disorders, particularly as there is a rapidly increasing prevalence of neurodegenerative and neurodevelopmental diseases.[1] The costs associated with developing neurotherapeutics is significant in large part due to the high rates of attrition in later stages of development.[2] The implementation of a low cost, predictive, and physiologically relevant *in vitro* screening model to more rigorously facilitate hit to lead candidate selection providing greater *in vivo* correlative rank ordering of potential compounds or drug delivery systems for further development is imperative.

Many have theorized that the high rates of attrition are predominantly due to the inability of drug candidates to cross the blood brain barrier (BBB).[1–3] The BBB has traditionally been viewed as the brain microvessel endothelial cells (BMECs) that line the capillaries of the brain to maintain a homeostatic environment. The

BBB separates the brain parenchyma from the systemic circulation and prevents permeation of potential xenobiotics into the brain interstitial fluids.[4,5] The BBB endothelium is unique in comparison to the periphery due to the high expression of efflux proteins, drug transporters, metabolizing enzymes, and the presence of restrictive tight junctions.[6,7] Tight junctions in the brain are formed between adjacent BMECs by a complex of transmembrane intracellular cleft spanning proteins such as the occludins and claudins 3 and 5, which anchor to cytosolic scaffolding proteins supported by the actin cytoskeleton.[8–10] The presence of restrictive tight junctions limits the permeation of small hydrophilic compounds, forcing compounds to move transcellularly in order to cross the BBB.

The high expression levels of non-substrate specific ATP-binding cassette (ABC) transporters such as P-glycoprotein (P-gp) and Breast Cancer Resistance Protein (BCRP) results in a high degree of efflux for molecules that attempt to cross the BBB through the transcellular pathway.[11] The presence of efflux transporters may limit the permeation of potential neurotoxicants, while also presenting a challenge for drug delivery as a number of intended neurotherapeutics tend to be lipophilic, favoring multidrug-resistant isoform efflux.[12] Due to their unique presence in the BBB, restrictive tight junctions and functional efflux proteins are key validation characteristics when establishing an *in vitro* BBB screening model.

The *in vivo* BBB phenotype is also largely modulated by the presence of supporting cellular and non-cellular components including astrocytes, pericytes, neurons, and the basal lamina. Together, these components make up the neurovascular unit (NVU), which are each essential for the function of the BBB *in vivo*. Astrocytes are a glial cell type that fully surround the endothelium and are linked to each other via gap junctions.[13] Single astrocytes have been shown to interact with up to four different neurons and five blood vessels, making them the cellular link between the endothelium and brain parenchyma.[14–16] Astrocytes participate in ion and water regulation due to the localization of aquaporin 4 and ion channels in the astrocytic end-feet and have been linked to the secretion of basal lamina proteins.[10,17] Additionally, astrocytes influence BMEC growth, modulation through extracellular signaling, play an important metabolic role, and assist in the functional maintenance through the secretion of soluble factors which have been shown to be essential for NVU homeostasis.[18–21] Towards the latter point, several *in vitro* and *in vivo* studies have demonstrated that changes in BBB integrity may result from a deficiency of certain astrocytic soluble factors.[18–21]

Pericytes are found enveloped in the basal lamina of the NVU between the astrocytes and endothelium. However, pericyte distribution is not continuous and in general cover approximately one third of the BMEC basal layer, with higher densities observed regiospecifically within the brain.[22] Pericytes are believed to play a similar role as astrocytes in NVU modulation through the secretion of soluble factors, but are unique in their role in NVU formation and maintenance, specifically during development.[23,24] Pericyte-endothelial crosstalk occurs through a number of signal cascades including platelet-derived growth factor B (PDGF-B) and transforming growth factor-β (TGF-β), as well as others.[25] Interactions between the pericytes and endothelium occurs within the basal lamina due to the relative location of embedded pericytes in the shared basement membrane, potentially suggesting that the composition of the extracellular matrix plays a role in BBB development and maintenance. The basal lamina is a non-cellular component of the NVU and is responsible for maintaining integrity of the BBB by anchoring the cellular components. There are a significant number of basement membrane proteins that include fibronectin, collagen IV, laminins, and vitronectin that form the matrix which is approximately 20nm thick *in vivo*.[6,26,27] Given the multiple components that make up the NVU, cellular and non-cellular, we propose that the BBB should be viewed as the directly interacting BMECs, pericytes and astrocytes of the NVU as a whole rather than simply the contributions of the BMECs.

Since its establishment in 2005, the hTERT oncogene and SV40 immortalized human cerebral microvessel endothelial cell line (hCMEC/D3) developed from primary endothelial cells of an epilepsy patient has been the most widely used immortalized endothelial cell line for BBB *in vitro* models.[28,29] Although it is widely used, studies (as well as our observations, unpublished results) have revealed that hCMEC/D3 cells can have relatively "leaky" tight junctions and demonstrate a functional reduction in efflux transporter expression with passaging.[30–33] An alternative immortalized human brain endothelium is the HBEC-5i cell line that was singly transfected with SV40 and originates from a patient pool of cerebral cortex fragments, lacking pathological abnormalities.[34,35] The HBEC-5i has been used predominantly in the study of cerebral malaria; however, these studies have established the potential for this cell line to be used for BBB *in vitro* permeability screening.[35–38] These cells have been observed to express a high number of electron-dense tight junctions as seen under electron scanning microscopy, as well as provide high transendothelial electrical resistance (TEER) and low permeability comparable to other immortalized BMECs.[35] Recently, the HBEC-5i cell line has been used for *in vitro* modeling of the BBB showing functional expression of ABC transporters and stable barrier properties over multiple days of culture, suggesting they are a viable alternative to the hCMEC/D3 cell line and other immortalized BMEC sources.[39,40]

Given the interaction of multiple cell types that maintain the BBB phenotype in the NVU, many *in vitro* models include astrocytes and pericytes in conjunction with BMECs.[30,41–45] Typically, these models involve seeding the endothelium on the apical surface of the filter and the supporting astrocytes and pericytes in the basolateral chamber or on the reverse side of the filter.[46–50] In this study we have further developed and optimized our previously established direct contact, layered coculture model to form a triculture system with the inclusion of pericytes to further increase the physiological relevance of the *in vitro* model.[51] The direct contact, layered triculture model is cultured by seeding astrocytes, followed by pericytes, then the endothelium all on the apical side of a filter support to reflect the *in vivo* configuration and cell-cell contacts of the BBB in the *in vivo* NVU (Figure 1). In our previous studies, we have utilized a One Factor at a Time approach to optimize culturing variables in a laborious and time-consuming manner. Given the multiple factors that influence the performance of this model, we have now utilized a design of experiments (DOE) approach to determine optimal culturing conditions by assessing the influence of multiple variables on barrier properties in a single experiment. This study has demonstrated that a DOE based approach, typically utilized in non-biological process optimization, can be used to optimize other multi-factor cell-based *in vitro* systems by assessing variable influence on model performance. Additionally, the results of this study demonstrate the importance of direct cell contact in *in vitro* models and suggests that increasing physiological relevance of *in vitro* models to mimic the *in vivo* NVU BBB can further enhance screening tools for neurotherapeutic development.

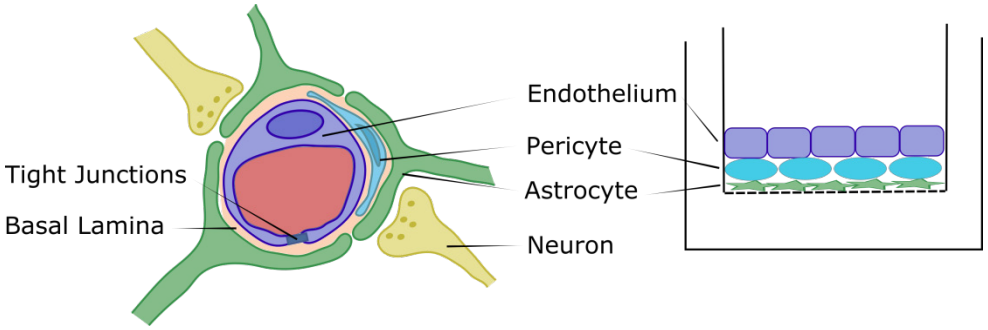

Figure 1 Cross sectional depiction of the Blood-Brain Barrier within the neurovascular unit (NVU) with the endothelium (BMECs) lining the capillary, pericytes embedded within the basal lamina, astrocytes having nearly full coverage of the BMECs and surrounding pericytes, and neurons in close contact with the astrocytes (left). The direct contact triculture model on the apical surface of a Transwell® filter support mimicking the *in vivo* NVU. Astrocytes are seeded first on the filter, followed by pericytes, then BMECs to generate a fully apical, direct contact triculture model (right).

Methods

Materials

Transwell® filters of 12 mm 0.4 µm pore size, T-75 culture flasks, Matrigel®, mouse laminin, and type I rat tail collagen were purchased from Corning (Corning, NY, USA). Hank's balanced salt solution (HBSS) and Dulbecco's Modified Eagle Medium/Nutrient Mixture F-12 (DMEM/F-12) were obtained from Gibco (Carlsbad, CA, USA). Fetal bovine serum (FBS), hydrocortisone, lithium chloride, retinoic acid, rhodamine 123 (R123), elacridar, digoxin, carbamazepine, colchicine, clozapine, caffeine, and prazosin hydrochloride were purchased from MilliporeSigma (St. Louis, MO, USA). HEPES (2-[4-(2-hydroxyethyl)piperazin-1-yl]-ethanesulfonic acid) and calcium chloride dihydrate were obtained from J.T. Baker (Phillipsburg, NJ, USA). Dexamethasone was obtained from MP Biomedicals (Santa Ana, CA, USA). Endothelial cell growth supplement (ECGS) was purchased from Alfa Aesar (Haverhill, MA, USA). Fluorescein isothiocyanate (FITC) labeled 4 kD dextran was purchased from Chondrex (Redmond, WA, USA). Poly-L-lysine (PLL) was purchased from Trevigen (Gaithersburg, MD, USA). Radiolabeled compounds [14C]-mannitol, -sucrose, -inulin, -PEG-4000, and [3H]-L-histidine were purchased from Moravek Biochemicals Inc. (Brea, CA, USA). Human astrocytes, human brain vascular pericytes, astrocyte medium, pericyte medium, and astrocyte and pericyte growth factors were all obtained from ScienCell Research Laboratories (Carlsbad CA, USA). HBEC-5i cells were purchased from ATCC (Manassas, VA, USA).

Cell culture

Human Brain Endothelial Cells (HBEC-5i) were maintained in T-75 culture flasks pre-coated with Type I rat tail collagen with medium changes every 3 days and culturing at 80-90% confluency. The cells were utilized in the studies between passages 22 and 30. HBEC-5i culture medium was made up of Dulbecco's Modified Eagle Medium/Nutrient Mixture F-12 (DMEM/F-12) supplemented with 10% FBS, 15mM HEPES, and 40µg/mL endothelial cell growth supplement (ECGS). Human astrocytes and human brain vascular pericytes are maintained in T-75 culture flasks pre-coated with poly-L-lysine with medium changes every 3 days and subculturing at 80-90% confluency. For the studies presented herein, the astrocytes and pericytes were utilized between passage 4 and 10. Astrocyte culture medium was made up of Astrocyte Medium supplemented with 5% FBS, astrocyte growth supplement, and penicillin/streptomycin. Pericyte culture medium was made up of Pericyte Medium supplemented with 5% FBS, pericyte growth supplement, and penicillin/streptomycin.

Experimental design for optimization

Optimization of plating conditions (cell seeding densities, extracellular matrix protein, and length of culture) and medium additives were performed in sequential design of experiment (DOE) analyses. For plating studies JMP® 13.2 from SAS statistical software was used to determine the plating conditions of each experimental run for a total of 39 combinations by utilizing a 5 factor, 2 level, custom design (DOE_P). Each run was done in a single replicate with DOE_P selected conditions to determine best levels for each variable and then the combined optimized conditions were further confirmed in subsequent experiments in triplicate. Table 1 lists the various factors and the respective levels of each.

Table 1 Plating factors and conditions for DOE (DOE_P)

Factor	Selected Range*
Astrocyte Seeding Density	20,000 – 60,000 cells/cm^2
Pericyte Seeding Density	20,000 – 60,000 cells/cm^2
HBEC-5i Seeding Density	50,000 – 110,000 cells/cm^2
Study Day	Day 5 – 9
Extracellular Matrix	Collagen I, Matrigel, Laminin

*3 levels each factor

Similarly, medium optimization was performed in two analyses using a custom design DOE to determine medium conditions that resulted in the tightest barrier properties. The first analysis (DOE_{M1}) was performed using HEPES, hydrocortisone, dexamethasone, LiCl, calcium, and retinoic acid, using the selected date for permeability analysis at 9 days post endothelial cell plating (Table 2). A second analysis (DOE_{M2}) was performed, based on the results of the first, using hydrocortisone, dexamethasone, LiCl, and retinoic acid at both 5 and 7 days post endothelial cell plating (Table 3).

Table 2 Medium optimization with evaluation on Day 9 (DOE_{M1})

Factor	Selected Range*
HEPES	15 – 25mM
Hydrocortisone	0 – 1.4µM
Dexamethasone	0 – 10µM
Lithium Chloride	0 – 10mM

Citation: Lubin KE, Knipp GT. Design of experiment based optimization of an *in vitro* direct contact triculture blood brain barrier model for permeability screening. *Pharm Pharmacol Int J.* 2021;9(4):143–158. DOI: 10.15406/ppij.2021.09.00340

Table Continued...

Factor	Selected Range*
Calcium	0 – 1mM
Retinoic Acid	0 – 10μM
Study Day	Day 9

*2 levels each factor (presence or absence of given additive)

Table 3 Medium optimization with evaluation on Day 5 and 7 (DOE_{M2})

Factor+	Selected Range*
Hydrocortisone	0 – 1.4μM
Dexamethasone	0 – 10μM
Lithium Chloride	0 – 10mM
Retinoic Acid	0 – 10μM
Study Day	Day 5 or 7

+All medium supplemented with 15mM HEPES

*2 levels each factor (presence or absence of given additive)

Plating direct contact triculture on tanswell® filter support

For the DOE_p studies, filters were pre-coated with poly-L-lysine (PLL) by pre-coating 12mm, 0.4μm pore Transwell® inserts with 5μg/cm^2 PLL. Astrocytes were plated at seeding densities of 20,000, 40,000, or 60,000cells/cm^2 and allowed to grow for 48 hours. After 48 hours of astrocyte growth, astrocyte medium was removed and pericytes were seeded atop the astrocyte lawn at seeding densities of 20,000, 40,000, or 60,000cells/cm^2 and allowed to grow for 48 hours. After 48 hours of pericyte growth, apical medium was replaced with the specified ECM protein solution. Astrocyte-pericyte lawn filters were coated with one of the following ECM proteins at the respective concentrations: Matrigel® 25μL/cm^2 (2.5μg/cm^2), Laminin 5μg/cm^2, or Type I Rat Tail Collagen 5μg/cm^2. To coat inserts, Matrigel®, Laminin, or collagen I aliquots were diluted in HBSS with Ca^{2+} and Mg^{2+} and 0.5mL dispensed onto to each respective 12mm insert and left to incubate with the respective ECM protein for 45min at 37°C. After incubation, the ECM solution was removed and HBEC-5i cells were plated at seeding densities of 50,000, 80,000, or 110,000 cells/cm^2 and allowed to grow for 5, 7, or 9 days prior to permeability measurements. Cultures were maintained in complete HBEC-5i medium with medium changes every other day following endothelial cell plating. Transendothelial electrical resistance (TEER) was measured every 24 hours after HBEC-5i plating using a 4mm Chopstick electrode with EVOM2 Volt/Ohm Meter (World Preclinical Instruments), and normalized based on resistance across blank filter supports.

In $DOE_{M1/2}$ studies, the culturing methodology described above was used with the modification that the complete HBEC-5i culture medium was supplemented with the DOE selected factors and introduced to cultures 24 hours post endothelial plating with medium changes every other day until the day of study. Medium for $DOE_{M1/2}$ was prepared from concentrated stock solutions of 1 M HEPES in water, 4.6mM hydrocortisone in ethanol, 3.8mM dexamethasone in DMSO, 11.8 M LiCl in water, 1.7 M $CaCl_2$ in water, and 33.3mM retinoic acid in DMSO. Final solvent content was normalized across all runs to eliminate solvent effect as a confounding factor in the study.

Plating monoculture and direct contact coculture on transwell® filter support

Monoculture (HBEC-5i alone) and direct contact coculture (astrocyte-HBEC-5i and pericyte-HBEC-5i) models were used for comparison with the DOE optimized direct contact triculture. For monoculture studies, 12mm, 0.4μm pore Transwell® inserts were pre-coated with 25μL/cm^2 Matrigel®. HBEC-5i cells were plated on Matrigel® coated filters at a density of 80,000cells/cm^2 and cultured for 9 days with medium changed every other day. Direct contact cocultures were plated according to methods developed by Kulczar et al. with some modifications.[51] Transwell® filters were pre-coated with 5μg/cm^2 PLL followed by seeding of astrocytes or pericytes at 20,000cells/cm^2 and allowed to grow for 48 hours. At 48 hours post astrocyte or pericyte plating, HBEC-5i cells at 80,000cells/cm^2 were seeded directly atop the lawn of pre-seeded cells and cultured for an additional 9 days with medium changed every other day.

Permeability assays

To optimize conditions, permeability was measured using 4kD FITC-dextran at an initial concentration of 0.25mg/mL in HBSS with Ca^{2+} and Mg^{2+}. Triculture DOE generated plating conditions and the optimized parameters were washed and left to equilibrate in HBSS at 37°C for 30 minutes prior to the start of the permeability assay. Permeability was performed at 37°C on a rocking platform maintaining sink conditions and sampling at 15, 30, 45, 60, and 90 minutes. Samples of 100μL from each basolateral chamber were removed at each time point and placed into a 96-well black flat-bottomed well plate for fluorescence reading. After sampling, naïve HBSS was added back to the basolateral chamber to maintain hydrostatic pressure and the lost mass was accounted for in the calculated permeation rates. Samples were analyzed using a BioTek Synergy 4 plate reader at excitation of 485nm and emission of 530nm. Apparent permeability (P_{app}) was calculated using equation 1 (eq. 1)

$$P_{app} = \frac{dM/dT}{C_0 \times A} \quad \text{(eq. 1)}$$

where dM/dT is the amount of Dextran that moves across the filter over time, Co is the initial concentration in the donor (apical) chamber, and A is the surface area of the filter support. The effective permeability (P_{eff}, permeability contributions of cell layer alone) of each condition was determined using equation 2 (eq. 2) where the P_{filter} value used is that of the ECM used in the given condition.

$$\frac{1}{P_{app}} = \frac{1}{P_{eff}} + \frac{1}{P_{filter}} \quad \text{(eq. 2)}$$

Apparent permeability of additional paracellular markers of varying sizes ([^{14}C]-mannitol, [^{14}C]-sucrose, [^{14}C]-inulin, and [^{14}C]-PEG-4000) was determined in the optimized direct contact triculture. Permeability assays were performed as stated above with an initial concentration of 0.25μCi/mL in HBSS for all markers and analysis performed utizing a liquid scintillation counter.

A range of BBB positive and negative permeants were used to further evaluate barrier properties of the optimized model. The permeability of [^{3}H]-L-histidine, carbamazepine, colchicine, digoxin, clozapine, and prazosin was determined by preparing 10mM stock solutions of each compound in DMSO, with the exception of [^{3}H]-L-histidine. For each study, the final concentration of DMSO was equivalent at 1% (v/v). Permeability of [^{3}H]-L-histidine was determined using the

same method as stated above for radiolabeled paracellular markers. Working solutions of non-radiolabeled compounds were prepared at a concentration of 25µM in HBSS with permeability measurements performed as stated above and sampling at 30, 60, 90, 120, and 150 minutes. Analysis for these compounds was performed using high performance liquid chromatography (HPLC). Permeability was calculated according to equation 1.

The function of P-gp in the triculture model was determined using P-gp substrate rhodamine 123 (R123) in the presence and absence of the inhibitor elacridar. Stock solutions of R123 (2mM) and elacridar (10mM) were prepared in DMSO. Working solutions of 10µM R123 and 2µM elacridar were prepared in HBSS with 1% DMSO. For inhibition studies, tricultures plated on permeable filter supports were pre-incubated with 2µM elacridar for 45 minutes prior to the addition of R123. Samples were removed at 30, 60, 90, and 120 minutes and analysis was performed using the BioTek Synergy 4 plate reader at excitation of 485nm and emission of 530nm. Permeability was calculated according to equation 1.

High performance liquid chromatography

Analysis of carbamazepine, caffeine, colchicine, digoxin, clozapine, and prazosin was performed on an Agilent 1100 reverse phase HPLC with variable wavelength detection (VWD), as briefly described below and summarized in Table 4.

Table 4 High Performance Liquid Chromatography analyses performed on an Agilent 1100 reverse phase HPLC with variable wavelength detection (VWD)

Compound	Column temperature	Mobile phase (water:acetonitrile)	Flow rate (mL/min)	Absorbance measurement (nm)
Caffeine	ambient	90:10:00	1	275
Carbamazepine	40°C	65:35:00	1.5	284
Clozapine	40°C	45:55:00	1.5	254
Colchicine	40°C	75:25:00	1.5	354
Digoxin	40°C	70:30:00	1.1	218
Prazosin	40°C	65:35:00	1.5	254

All samples were run isochratically through an Ascentis® C-18 15 x 4.6mm, 5µm column, at 25µL injection volume, using water and acetonitrile (ACN) for all mobile phase

Statistical analysis

Custom experimental designs based on categorical and discrete continuous factors were generated by JMP 13.2 statistical software. Analysis of each DOE was done by fitting models based on the P_{eff} of 4kD dextran response to standard least squares to determine optimal conditions. In comparison studies, all conditions were performed in triplicate (n=3) and subjected to Student's *t*-test or one-way ANOVA with Tukey Kramer post-hoc test. A p-value of 0.05 was considered to be statistically significant.

Results

Plating optimization (DOE_P)

Traditionally, a One-Factor-at-a-Time (OFAT) approach is used to assess the impact of variable changes in cell-based models and processes, where one variable (e.g., cell density) is optimized in the presence of several other unoptimized variables that result in an inefficient and laborious manner. A Design of Experiments (DOE) based approach allows for the influence of multiple factors to be observed on a measured response to arrive at an optimal level for each given variable. Furthermore, it allows one to more rapidly identify optimized growth conditions in a time and labor efficient manner. Our previous studies towards establishing a direct contact triculture (unpublished results) and our direct contact coculture model, were used to inform our selection of respective seeding densities for all three cell types, ECM used to aid endothelial attachment, and length of culture of the endothelium that consisted of the initial selected factor ranges.[51] Optimal plating conditions were determined using P_{eff} values to account for the differences associated with ECM coatings. Conditions 8 (60 HA, 60 HBVP, 110 EC, Laminin, Day 9) and 20 (20 HA, 20 HBVP, 110 EC, Laminin, Day 9) exhibited the lowest Peff values at 3.2 x 10^{-6}cm/sec (Figure 2). Condition details and tabulated P_{eff} data of DOE_P are noted in Supplemental Table 1.

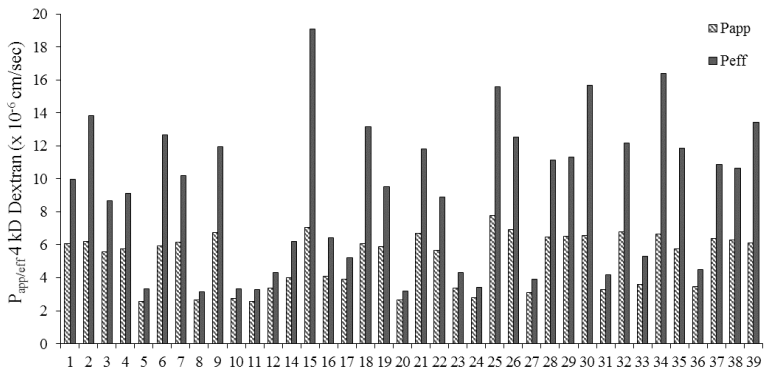

Figure 2 P_{app} and P_{eff} of 4 kD FITC-Dextran across different direct contact triculture conditions of DOE_P. All DOE_P selected conditions were performed as n=1 for a rapid evaluation of the different parameter combinations. Condition 13 was compromised and permeability was not performed, data point was excluded from statistical analysis.

Citation: Lubin KE, Knipp GT. Design of experiment based optimization of an *in vitro* direct contact triculture blood brain barrier model for permeability screening. *Pharm Pharmacol Int J.* 2021;9(4):143–158. DOI: 10.15406/ppij.2021.09.00340

Supplemental Table 1 Conditions and P_{eff} of 4kD Dextran of DOE_P

Condition	HA (cells/cm²)	HBVP (cells/cm²)	HBEC-5i (cells/cm²)	ECM	Day	P_{eff} (cm/sec)
1	40000	20000	110000	Collagen	7	9.99E-06
2	60000	20000	80000	Matrigel	5	1.38E-05
3	60000	20000	110000	Laminin	5	8.69E-06
4	60000	20000	110000	Laminin	5	9.14E-06
5	20000	20000	80000	Collagen	9	3.32E-06
6	20000	60000	50000	Matrigel	5	1.26E-05
7	60000	60000	80000	Collagen	7	1.02E-05
8	60000	60000	110000	Laminin	9	3.17E-06
9	60000	20000	50000	Collagen	5	1.19E-05
10	20000	60000	50000	Laminin	9	3.32E-06
11	20000	20000	50000	Matrigel	9	3.30E-06
12	20000	40000	110000	Matrigel	9	4.31E-06
13	20000	20000	110000	Collagen	5	-
14	60000	20000	110000	Collagen	9	6.19E-06
15	40000	20000	50000	Matrigel	5	1.91E-05
16	40000	60000	80000	Matrigel	9	6.43E-06
17	60000	60000	50000	Matrigel	9	5.22E-06
18	20000	20000	110000	Matrigel	5	1.32E-05
19	60000	60000	110000	Collagen	5	9.54E-06
20	20000	20000	110000	Laminin	9	3.20E-06
21	60000	60000	50000	Laminin	5	1.18E-05
22	20000	60000	110000	Laminin	5	8.87E-06
23	40000	40000	50000	Collagen	9	4.32E-06
24	20000	60000	110000	Collagen	9	3.40E-06
25	20000	20000	50000	Laminin	5	1.56E-05
26	20000	20000	50000	Collagen	7	1.25E-05
27	60000	20000	110000	Matrigel	9	3.91E-06
28	20000	60000	110000	Laminin	5	1.12E-05
29	20000	40000	80000	Collagen	5	1.13E-05
30	60000	60000	110000	Matrigel	5	1.57E-05
31	20000	60000	50000	Laminin	9	4.17E-06
32	20000	60000	50000	Collagen	5	1.22E-05
33	60000	20000	50000	Laminin	9	5.32E-06
34	60000	40000	50000	Matrigel	7	1.64E-05
35	20000	60000	110000	Matrigel	7	1.19E-05
36	60000	60000	50000	Collagen	9	4.47E-06
37	40000	40000	80000	Collagen	7	1.08E-05
38	40000	40000	80000	Laminin	7	1.06E-05
39	40000	40000	80000	Matrigel	7	1.34E-05

Citation: Lubin KE, Knipp GT. Design of experiment based optimization of an *in vitro* direct contact triculture blood brain barrier model for permeability screening. *Pharm Pharmacol Int J.* 2021;9(4):143–158. DOI: 10.15406/ppij.2021.09.00340

Based on the data trends, the culture length between the assay day was determined to have the largest impact on paracellular permeability resulting in significantly lower 4kD dextran permeability at day 9 compared to days 5 and 7. When separating the data by study day and factor there are observable trends in permeability coefficients among the factors including the effects of astrocyte and pericyte cell density. With extended culturing, higher seeding densities of astrocytes and pericytes result in higher permeability of the dextran (Figure 3). HBEC-5i seeding density also shows trends towards lower permeability at higher seeding densities; however, this trend is not as strong at day 9 when the cells have had sufficient time to reach confluence and have a longer time to differentiate.

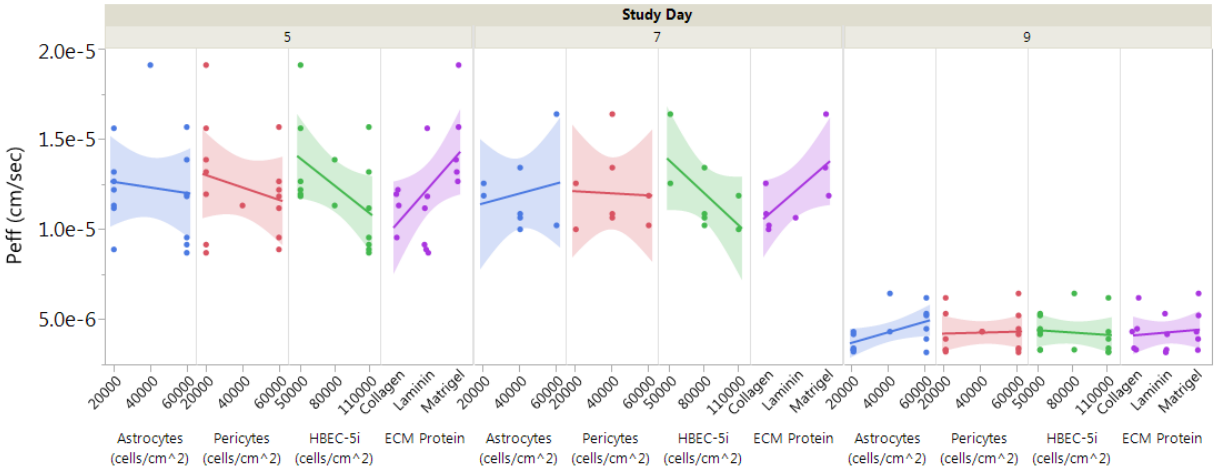

Figure 3 P_{eff} of 4 kD FITC-Dextran for DOE_P separated by factor and further by day of study showing relative trends of factor levels at increasing length of culture. All conditions are represented by single data points across the graph, n=1.

Using JMP 13.2 software, a prediction profiler was generated based on the obtained P_{eff} values for the given conditions. By maximizing Desirability to achieve the lowest possible permeability, the optimal conditions were determined to be 20,000cells/cm^2 for both astrocytes and pericytes, 80,000cells/cm^2 HBEC-5i cells, Matrigel® as the ECM protein, and culturing for 9 days post endothelial cell plating (Figure 4). These conditions would optimally generate a predicted P_{eff} value of 2.4 x 10^{-6}cm/sec for 4kD dextran. Upon repeating the analysis at selected optimal conditions, the P_{eff} of a 4kD dextran showed to be reproducible resulting in a similar permeability value (P_{eff}; 3.7 x 10^{-6}cm/sec±0.04, n=3).

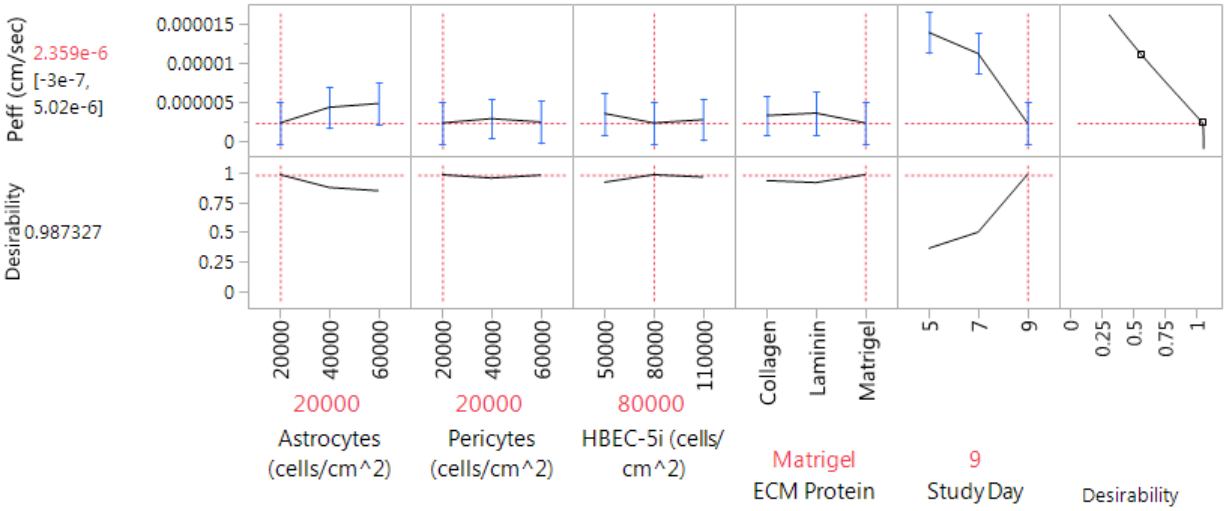

Figure 4 JMP 13.2 Prediction Profiler generated based on maximizing desirability for P_{eff} based on DOE_P. Optimal plating conditions 20,000 cells/cm^2 astrocytes and pericytes, 80,000 cells/cm^2 HBEC-5i, Matrigel, and 9 days of endothelial growth. Predicted P_{eff} of 2.4 x 10^{-6} cm/sec for optimal conditions.

Medium optimization ($DOE_{M1/2}$)

Selection of medium additives was based on literature and previous studies in our laboratory for HBEC-5i medium based on their reported influences on barrier tightness both *in vitro* and *in vivo*.[51–58] The first DOE analysis of medium variables aimed towards optimization (DOE_{M1}) was performed with the DOE_P optimized plating conditions of 20,000 cells/cm^2 for astrocytes and pericytes, 80,000 cells/cm^2 HBEC-5i, Matrigel, after 9 days of endothelial growth. HEPES, hydrocortisone, dexamethasone, lithium chloride, calcium, and retinoic acid were used as medium additives due their reported influence on tight junction expression and induction of

barrier properties in *in vitro* BBB models. The lowest achieved 4kD dextran P_{eff} of DOE_{M1} was 6.3 x 10^{-6}cm/sec, suggesting that, under these conditions, the additives did not provide further tightening of the model. Significant trends are not apparent for any of the additives with the exception of higher levels of HEPES resulting in higher permeability values. Given that many of these additives increased expression and differentiation of the endothelial cells, their effects on barrier properties were assessed at earlier days of culture. The optimal medium condition was determined to be 15mM HEPES, 1mM calcium, and 10µM retinoic acid, but the influence of these factors on barrier tightness was not significant (Figure 5). The full data set of DOE_{M1}, including medium conditions and P_{eff}, is tabled in Supplemental Table 2.

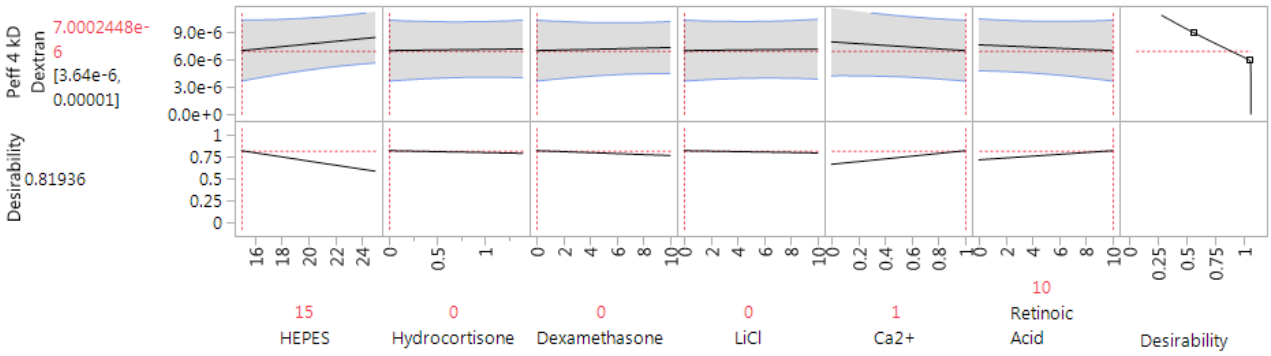

Figure 5 JMP 13.2 Prediction Profiler generated based on maximizing desirability for P_{eff} of DOE_{M1}. Optimal medium conditions 15 mM HEPES, 1 mM Ca^{2+}, and 10µM retinoic acid at 9 days of endothelial growth. Predicted P_{eff} of 7.0 x 10^{-6} cm/sec for optimal conditions.

Supplemental Table 2 Conditions and P_{eff} of 4kD Dextran of DOE_{M1}

Condition	HEPES (mM)	HC (µM)	DEX (µM)	LiCl (mM)	Ca^{2+} (mM)	RA (µM)	P_{eff} (cm/sec)
1	25	0	0	10	1	0	8.66E-06
2	15	1.4	10	10	1	10	9.12E-06
3	25	1.4	10	0	0	10	1.11E-05
4	15	0	0	0	1	0	7.29E-06
5	25	0	10	10	0	0	8.37E-06
6	25	0	10	10	1	10	1.07E-05
7	15	0	0	10	1	10	-1.87E-04
8	15	0	10	10	1	0	3.67E-05
9	15	0	0	10	0	0	1.20E-05
10	25	1.4	0	0	0	0	1.18E-05
11	25	0	10	0	1	0	1.09E-05
12	15	1.4	10	0	1	0	9.10E-06
13	15	1.4	10	10	0	0	7.10E-06
14	25	0	0	0	0	10	8.54E-06
15	15	0	10	0	0	0	1.66E-05
16	25	1.4	0	0	1	10	6.32E-06
17	25	1.4	0	10	0	10	1.10E-05
18	15	0	10	10	0	10	7.70E-06
19	25	1.4	10	10	1	0	1.82E-05
20	25	1.4	0	10	0	10	9.79E-05
21	15	1.4	0	10	1	0	7.29E-06
22	20	0.7	5	5	0.5	5	6.71E-06
23	15	1.4	0	0	0	10	2.00E-05
24	15	0	10	0	1	10	6.87E-06

Citation: Lubin KE, Knipp GT. Design of experiment based optimization of an *in vitro* direct contact triculture blood brain barrier model for permeability screening. *Pharm Pharmacol Int J.* 2021;9(4):143–158. DOI: 10.15406/ppij.2021.09.00340

Based on these results a second analysis (DOE_{M2}) was performed to assess the influence of the additives in earlier days of culture. These studies were conducted in the presence or absence of hydrocortisone, dexamethasone, lithium chloride, and retinoic acid at 5 and 7 days post endothelial cell culture, HEPES was held constant at 15mM and calcium was removed from DOE_{M2}. The lowest 4kD dextran P_{eff} of DOE_{M2} was 8.3 x 10^{-6}cm/sec, suggesting that the additives do not provide increased barrier tightness based on the optimized plating conditions of DOE_{P}. Optimal conditions for medium was determined to be 10µM dexamethasone, 10µM retinoic acid, 10mM LiCl, through 7 days of endothelial cell culture; however, these conditions were not used for continued assessment of the optimized model due to the lack of improvement over unmodified medium (Figure 6). The complete data set of DOE_{M2}, including individual run and P_{eff} results, can be found in Supplemental Table 3.

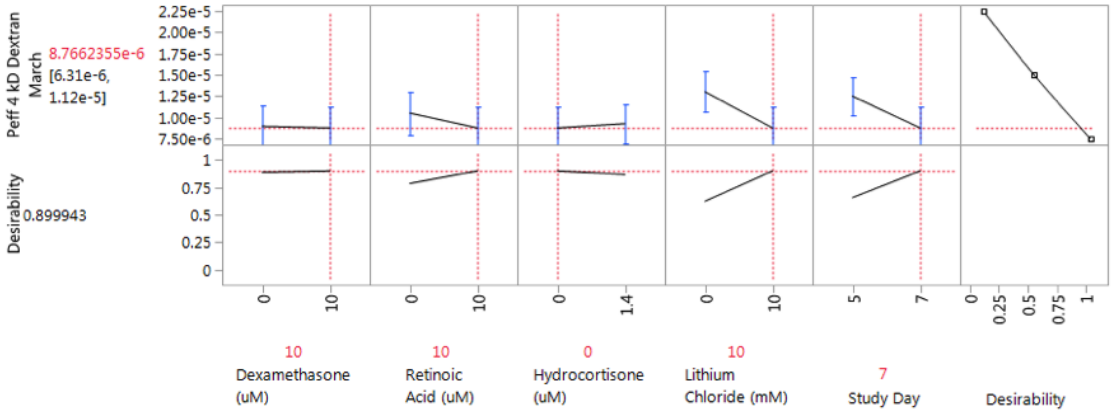

Figure 6 JMP 13.2 Prediction Profiler generated based on maximizing desirability for P_{eff} of DOE_{M2}. Optimal medium conditions 10µM dexamethasone, 10µM retinoic acid, 10mM LiCl, through 7 days of endothelial culture. Predicted P_{eff} of 8.8 x 10^{-6} cm/sec for optimal conditions.

Supplemental Table 3 Conditions and P_{eff} of 4kD Dextran of DOE_{M2}

Condition	HC (µM)	DEX (µM)	LiCl (mM)	RA (µM)	Study Day	P_{eff} (cm/sec)
1	1.4	0	10	0	7	9.47E-06
2	0	0	0	10	5	1.91E-05
3	1.4	10	10	10	7	8.29E-06
4	1.4	10	0	10	5	2.07E-05
5	1.4	10	0	0	7	1.47E-05
6	0	0	10	10	7	1.17E-05
7	1.4	10	10	0	5	1.65E-05
8	1.4	0	0	0	5	2.05E-05
9	0	0	0	0	7	1.33E-05
10	0	10	10	0	7	1.01E-05
11	1.4	0	10	10	5	1.08E-05
12	0	10	10	10	5	1.15E-05
13	1.4	0	10	10	5	1.16E-05
14	1.4	0	10	0	7	1.13E-05
15	0	10	0	10	7	1.08E-05
16	1.4	10	10	10	7	1.06E-05
17	1.4	10	0	10	5	1.31E-05
18	0	10	0	0	5	1.67E-05
19	1.4	10	10	0	5	1.72E-05
20	1.4	0	0	10	7	1.32E-05
21	0	10	10	10	5	1.32E-05
22	0	0	10	0	5	1.34E-05
23	1.4	10	0	0	7	1.68E-05
24	0	0	0	10	7	1.56E-05

Citation: Lubin KE, Knipp GT. Design of experiment based optimization of an *in vitro* direct contact triculture blood brain barrier model for permeability screening. *Pharm Pharmacol Int J.* 2021;9(4):143–158. DOI: 10.15406/ppij.2021.09.00340

Permeation comparisons to mono- and cocultures

The optimized direct contact triculture was compared to a monoculture of HBEC-5i cells alone and direct contact cocultures of HEBC-5i cells seeded atop a lawn of astrocytes or pericytes (Figure 7A). Effective permeability of the 4 kD FITC-dextran was used for comparison between the different models. In comparison to the optimized direct contact triculture (3.7 x 10^{-6}±0.0cm/sec) the HBEC-5i monoculture had the highest observed permeability (19.7 x 10^{-6}±3.0cm/sec; $p<0.01$), followed by the perictye-HBEC-5i coculture (15.1 x 10^{-6}±3.7cm/sec; $p < 0.05$), and the astrocyte-HBEC-5i coculture (12.8 x 10^{-6}±2.1cm/sec; $p<0.05$). Given the significant differences observed between the direct contact triculture and the monoculture and coculture models, the inclusion of all three cell types offers increased barrier tightness for the *in vitro* model.

Direct contact triculture BBB marker compounds

Paracellular markers possessing a broad range of hydrodynamic radii were used to evaluate the functional tightness of the optimized model (Figure 7B).[59–61] The lowest apparent paracellular permeability observed was that of PEG-4000 (7.85 x 10^{-6}±0.03cm/sec, 15.9Å) followed by inulin (P_{app}=15.53 x 10^{-6}±0.15cm/sec, 10Å), mannitol (P_{app}=19.88 x 10^{-6}±0.07cm/sec, 4.3Å), and sucrose (P_{app}=21.76 x 10^{-6}±0.17 cm/sec, 5.2Å). The apparent paracellular permeability of the hydrophilic markers shows the model is able to distinguish between markers of varying sizes. However, based on the hydrodynamic radius, sucrose should have a lower permeability as the larger compound in comparison to mannitol.

P-gp function in the direct contact triculture was assessed using P-gp substrate R123 alone and in the presence of P-gp inhibitor elacridar (Figure 7C). In the absence of inhibitor, the P_{app} of R123 was 18.52x10^{-6}±0.58cm/sec. The presence of elacridar significantly increased the P_{app} of R123 (P_{app}=21.14 x 10^{-6}±0.46 cm/sec; $p<0.01$) across the direct contact triculture. Additional P-gp substrates were utilized as marker compounds such as digoxin (P_{app} = 9.21 x 10^{-6}±0.31cm/sec) and colchicine (P_{app}=18.67 x 10^{-6}±2.75cm/sec). Prazosin, a BCRP substrate, was used to assess the function of other efflux transporters in the direct contact model (P_{app}=6.16 x 10^{-6}±0.11cm/sec) (Figure 7).

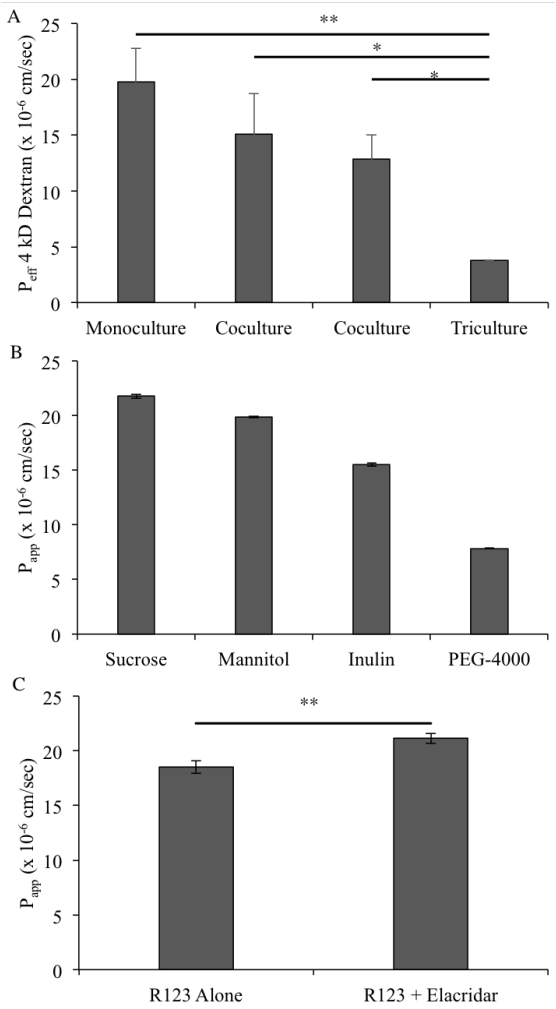

Figure 7 Optimized Triculture Permeability. (A) Effective permeability (P_{eff}) of 4 kD FITC-dextran across an HBEC-5i monoculture, pericyte-HBEC-5i direct contact coculture, astrocyte-HBEC-5i direct contact coculture, and optimized direct contact triculture. Statistical analysis was performed with one-way ANOVA and Tukey-Kramer post-hoc test. Error bars represent one standard deviation (n=3). *, $p < 0.05$ and **, $p < 0.01$. (B) Apparent permeability of radiolabeled paracellular markers [^{14}C]-sucrose. [^{14}C]-mannitol, [^{14}C]-inulin, and [^{14}C]-PEG-4000 across the optimized direct contact triculture. Error bars represent one standard deviation (n=3). (C) Apparent permeability of P-gp substrate rhodamine 123 (R123) in the presence and absence of P-gp inhibitor elacridar across the optimized direct contact triculture. Assays were run in triplicate and subjected to Student's *t*-test. Significant difference is indicated by *, $p<0.05$ and **, $p<0.01$. Error bars represent one standard deviation (n=3).

Citation: Lubin KE, Knipp GT. Design of experiment based optimization of an *in vitro* direct contact triculture blood brain barrier model for permeability screening. *Pharm Pharmacol Int J.* 2021;9(4):143–158. DOI: 10.15406/ppij.2021.09.00340

The antipsychotic drug clozapine showed an apparent permeability value of 8.15 x 10^{-6}±0.58cm/sec. The amino acid L-histidine was used to assess facilitative transport across the *in vitro* model with an observed apparent permeability of 52.61 x 10^{-6}±0.70cm/sec, as reported previously.[60] Carbamazepine is an antiepileptic drug and a BBB positive permeant with an observed apparent permeability of 27.71 x 10^{-6}±1.13cm/sec in the optimized model. Caffeine, a small hydrophilic molecule, also had BBB positive permeation with an obtained apparent permeability of 28.93 x 10^{-6}±1.15cm/sec (Figure 8).

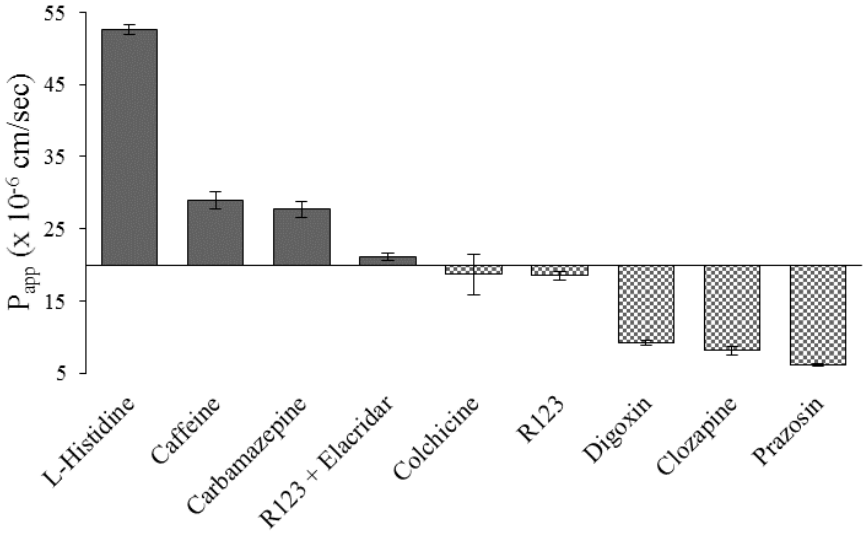

Figure 8 Apparent permeability of BBB positive (L-histidine, carbamazepine, and rhodamine 123 in the presence of P-gp inhibitor elacridar) and negative (colchicine, rhodamine 123, digoxin, clozapine, and prazosin) permeants across the optimized direct contact triculture. Assays were performed in triplicate. Error bars represent one standard deviation (n=3).

Discussion

In vitro screening models have traditionally been used to evaluate the potential of new chemical entities to cross the BBB, with much of the emphasis of these models being placed on the endothelial cell type. The BMEC used is often primary or immortalized and of animal or human origin, each presenting its own advantages for use in *in vitro* models.[30,62] Although animal sources are typically lower cost, have significantly higher access, and can be easier to isolate, physiological and phenotypic differences between the human and animal NVU make human cell sources preferred for drug permeability screening due to the presumed physiological relevance to the patient. Primary cells, directly isolated from patients, often present a phenotype most similar to *in vivo*, but are often difficult to acquire due to ethical reasons, require intricate isolation protocols, and present concerns with patient specific differences.[63,64] Therefore, much of the emphasis has been placed on establishing and characterizing human immortalized cell lines for robust screening methods.

The HBEC-5i cell line has not been as extensively used for *in vitro* BBB permeability modeling comparative to other BMEC cell sources (e.g., hCMEC/D3).[60] However, it has been shown to have good expression levels of brain endothelial markers such as vascular cell adhesion molecule (VCAM-1) and intercellular adhesion molecule (ICAM-1) essential for immune cell trafficking, CD51 (α_V-integrin) involved in extracellular matrix adhesion, as well as tight junction proteins zonula occluden 1 (ZO-1) and claudin-5.[35,39] Transporter expression and function of BCRP, P-gp, MRP-1, and MRP-2 has also been demonstrated recently to be comparable to other immortalized brain endothelium.[39] Conversely, this cell line has also been indicated to be lacking in expression of platelet endothelial cell adhesion molecules (PECAM-1 and CD31) and the macrophage scavenger receptor CD36.[35,65] Given the expression of endothelial markers and transporters that have been investigated by others, we selected the HBEC-5i cell line as the BMEC for the direct contact triculture rather than the hCMEC/D3 cell line we utilized in development of the direct contact coculture.[51]

In vitro models of the BBB are increasingly being developed to provide physiological relevance through co- and triculture indirect contact methods with astrocytes and pericytes that comprise the NVU to further enhance barrier properties. Seeding supporting NVU cells on the reverse side of the filter support displays improved barrier properties in the cultured BMECs by reducing the distance between the cell types and improving the BBB phenotype in the cultured endothelium.[50,66] However, the direct cell-cell contact is limited due to the thickness of the filter support and opposable culturing surfaces, where growth through the filter pores provides limited interaction. The direct cell-cell contacts of astrocytes and pericytes with the endothelium *in vivo* are often overlooked in these multi-cellular models that are currently utilized.[30,41–45] We have previously shown that direct contact between astrocytes and the endothelium in a coculture model increases the barrier properties compared to endothelial monocultures and indirect plating methods.[51] Although astrocytes are often used as a supporting cell in *in vitro* models, pericytes also play an important role in influencing and regulating the BBB phenotype through a number of signaling cascades.[24,67,68] Since each supporting cell acts in a functionally different manner on the BMECs, incorporating both astrocytes and pericytes in direct contact cell based models should better enable synergistic effects of the NVU to be represented *in vitro*.

A design of experiments approach was taken to develop and optimize the direct contact triculture in order to adequately understand the interactions each variable would have on the performance of the

model. As opposed to an OFAT approach, DOE takes into account the implications of changing multiple variables to come to optimal conditions in a significantly more efficient manner in terms of time invested and resources required. In optimizing the triculture, we arrived at optimal conditions with reproducible results in a time frame of two months as opposed to our previous OFAT optimization efforts that spanned the course of multiple years. The results of DOE_p revealed optimal plating conditions of 20,000cells/cm^2 for both astrocytes and pericytes, 80,000cells/cm^2 for HBEC-5i, Matrigel® as the ECM to promote endothelial adhesion, and culturing the endothelium for 9 days after seeding. The comparison of 4kD dextran permeability to other reported data revealed that our optimized model infers that the model is among the tightest we found reported, suggesting that culturing multiple NVU cell types in direct contact synergistically increases barrier tightness (Table 5).

Table 5 Peff Values of 4 kD Dextran (14 Å) for different BBB models

Model/Endothelial Cell Line	Peff (10^{-6} cm/sec)
DOE Direct Contact Triculture, HBEC-5i	3.7
Monoculture (HA conditioned medium), HBEC-5i	3.6[a]
Monoculture, hCMEC/D3	8.8[b], 5.4[c]
Isolated endothelial cells, rat	1.0[d]
In vivo microvessels, rat	0.92[e]

[a]Puech C, et al. Int J Pharm. 2018;551(1):281-289, [b]Förster C, et al. J Physiol. 2008;589(7):1937-1949, [c]Weksler B, et al. FASEB J. 2005;19(13):1872-1874, [d]Watson PMD, et al. BMC Neuroscience. 2013;14:59, [e]Yuan W, et al. Microvasc Res. 2009;77(2):166-173

In addition to selecting an optimized set of plating conditions, the DOE approach facilitated an understanding of how changing factor levels may impact model performance. At higher densities of astrocytes and pericytes, a decrease in paracellular tightness was observed with extended culture time. Length of culturing time will vary with each individual endothelial cell line seeded in combination with the astrocytes and pericytes in culture and should be optimized based on the increase in tightness as an indicator of differentiation. However, the endothelial culture times do need to take into account whether or not the co-cultured astrocytes and pericytes maintain viability or run the risk of becoming senescent at the latter stages of the study. Additionally, higher seeding densities of endothelial cells resulted in lower paracellular permeation rates at days 5 and 7, which may be expected by the increased ability of the cells to form a confluent layer at fewer days of culture. However, that trend is less drastic after 9 days of culture suggesting that seeding density does not play as significant of a role at confluency, but rather time in culture is necessary to allow for differentiation and adequate tight junction formation.

An effort to optimize culture medium (DOE_{M1} and DOE_{M2}) was made to further increase barrier properties of the model through the inclusion of additives that have been shown to enhance the BBB phenotype in *in vitro* and *in vivo* studies. Unmodified HBEC-5i medium contains 15mM HEPES; therefore, higher levels of HEPES were included to assess the impact of a higher buffering capacity on barrier tightness. Hydrocortisone was selected for its influence on inflammatory responses as a glucocorticoid and potential to prevent tight junction break down.[52] Lithium chloride has been shown to influence claudin expression through stimulation of the Wnt/β-catenin pathway.[53] Calcium was studied as a medium additive due to its influence on adherens and tight junction protein expression to increase barrier tightness, where studies have shown that low extracellular calcium levels can lead to an increase in paracellular permeability.[54,55] Like hydrocortisone, dexamethasone acts to inhibit inflammatory responses and upregulate tight junctions; however, it is a synthetic alternative to the naturally occurring hydrocortisone.[56] Lastly, retinoic acid is naturally secreted by glial cells and has revealed significant increases in paracellular tightness in *in vitro* BBB models.[57,58]

Between both assessments it was revealed that the length of culture time for the endothelium still had the largest impact on model performance regardless of additives (Figure 6). Based on this finding it is possible that due to the influence the additives have on the endothelium the HBEC-5i cells are differentiating before reaching confluency which is not sustainable through the length of culture. This phenomenon could also explain why the effects of additives appear to be more effective in DOE_{M2}, culturing for 5 or 7 days post endothelial plating, as the differentiation effects may be occurring earlier and not maintained through culture times for DOE_{M1}. A way to improve on this would be to include HBEC-5i seeding density as a factor in further assessments of medium additives. With the trends of DOE_p establishing the positive impacts higher seeding densities have on model tightness, seeding at a higher density (greater than the optimized 80,000cells/cm^2) with differentiation inducing medium supplements may result in the tightest barrier formed and additionally reduce culturing time. An alternative would be to continue with optimized conditions of DOE_p and include time of addition as a factor in further studies by introducing additives after the HBEC-5i have been in culture for more than 24 hours.

The influence of the medium additives may also extend beyond paracellular tightness. Hydrocortisone has been shown to increase barrier tightness through the upregulation of tight junction proteins, but has also been demonstrated to induce efflux transporter expression.[39,69,70] Expression and function of ABC efflux transporters, specifically BCRP and P-gp, was also demonstrated to be influenced by the release of tumor necrosis factor-α (TNF-α) and subsequent inflammatory responses.[39,70,71] However, hydrocortisone is a glucocorticoid that has been demonstrated to impact P-gp and BCRP expression by inducing anti-inflammatory responses. Therefore, in addition to the impact on paracellular tightness, the induction of efflux transporter expression should also be assessed by evaluating the time of addition of hydrocortisone to the culture medium.

The increase in physiological relevance of adding additional cell types of the NVU in direct contact with BBB endothelium provides increased barrier restrictive properties in comparison to the endothelium alone. Additionally, including both supporting cell types (astrocytes and pericytes) in direct contact with HBEC-5i cells results in increased barrier tightness compared to direct contact cocultures (astrocyte- or pericyte-HBEC 5i combinations alone). This finding suggests that including both the astrocytes and pericytes in *in vitro* models further synergistically enhances the properties of the BBB in addition to better representing the *in vivo* NVU. The inductive effects of astrocytes and pericytes and their roles in BBB maintenance have been well established; however, many of the models used for *in vitro* BBB permeability screening do not consider the direct contact the different cell types have with one another *in vivo*. By seeding astrocytes, pericytes, and the endothelium directly atop one another this model better mimics the 20 nm distance between the cell types due to the presence of the basal lamina that is seen *in vivo*.[22] Although indirect plating methods with cell types cultured on opposite sides of a 10μm thick filter support also provide increased barrier properties over endothelial monocultures, the direct contact triculture is more

physiologically relevant to the *in vivo* BBB that is observed in the NVU and does not require manipulation of the Transwell® system and potentially is more amenable to automation for higher capacity throughput screening assays.

Paracellular permeants of increasing hydrodynamic radius were selected to evaluate the tight junction formation in the direct contact model. With increasing marker size, there is a related decrease in paracellular permeability due to the size of the molecule in relation to the pore size of the tight junctions formed between adjacent endothelial cells. Permeability of [^{14}C]-PEG-4000 (15.9Å) is the lowest of all markers used as expected followed by [^{14}C]-inulin (10Å). In studies with the optimized direct contact triculture model, the permeability of [^{14}C]-sucrose (5.2Å) is faster than that of the smaller [^{14}C]-mannitol (4.3Å), which is opposite of what would be expected based on molecule size alone.[59–61] One possible explanation is that the relative size of the two markers is small in comparison to the paracellular pore radius in the triculture model, which would lead to issues in elucidating the differences in their respective permeation rates as they both traverse relatively fast. Alternatively, sucrose, a disaccharide of a fructose and glucose molecule linked via glycosidic bond, may serve as a substrate for active or facilitative nutrient transporters. For example, glucose permeation across the BBB has been reported to be modulated by several nutrient transporters, in particular the facilitative Glucose Transporter 1 (GLUT1) that is highly expressed in both BMECs and astrocytes.[72,73] Several neurotherapeutics utilize a pro-drug approach where the agent is conjugated to glucose in an effort to enhance brain parenchymal exposure via GLUT1.[72,74] Based on the structure of sucrose, the idea that there is some degree of nutrient transporter activity of the purported paracellular marker via the GLUT1 transporter is feasible. Therefore, we posit that the observed permeation rate for sucrose could be higher due to a potential transporter contribution that is not available for [^{14}C]-mannitol in the optimized direct contact triculture. This theory is further exacerbated by the presence of astrocytes and pericytes on the apical side of the Transwell® in the direct contact triculture since both of these cell types have reported expression of GLUT1. The potential for GLUT1 mediated transport and a potential increase the permeation of [^{14}C]-sucrose in the apical to basolateral direction in comparison to indirect *in vitro* models requires further investigation. Future studies might focus on delineating the effects GLUT1, a related transporter, with co-administration of transporter inhibitors, or with GLUT isoform transfected HBEC-5i cells.

The functional activity of ATP-Binding Cassette efflux transporters, with the most prevalent isoform being P-gp, in BMECs is a key characteristic of the *in vivo* BBB. P-gp, BCRP, and related multidrug resistance conferring efflux transporters function to prevent xenobiotics from permeating into the brain parenchyma with a broad substrate affinity and capacity. Rhodamine-123 (R123) is a commonly used P-gp substrate to assess functional activity in the presence or absence of an inhibitor. Elacridar is a third generation P-gp inhibitor and has been reported to have among the highest specificity and potency for P-gp inhibition within the class of agents.[75] We observed that the presence of elacridar resulted in an increase in R123 permeability across the direct contact triculture, suggesting that P-gp is functionally present in the optimized model. In these studies, R123 permeation was only assessed in the apical to basolateral direction. Additional studies to elucidate P-gp function can include bi-directional permeability assessment as well as cellular accumulation. However, given that P-gp is expressed in both the HBEC-5i and astrocyte cell types in direct contact, the assessment of P-gp function and expression would require more in depth studies focused on delineating the impact of P-gp in each cell and in combination. This is particularly true given the fact that astrocytes have also been reported to express P-gp, which may further obfuscate P-gp assessment of the endothelium alone.[76]

In addition to limiting paracellular permeation of hydrophilic solutes and potentially P-gp substrates, we theorized that a well-established *in vitro* model of the BBB found in the NVU should have an enhanced ability to differentiate between *in vivo* demonstrated high and low brain permeating compounds. *In vitro* permeability screening models capable of predicting *in vivo* permeation rates in order to rank new chemical entities is essential to facilitate compound advancement with translation as the aim.[77,78] A number of positive and negative permeants were selected to assess the utility of the direct contact triculture. Amino acids and related analogues (e.g. γ-aminobutyric acid or GABA) play a critical role in maintaining brain homeostasis and modulating function. Here we selected L-histidine as an amino acid that is actively transported in a stereospecific manner across the BBB by amino acid transporters and potentially Peptide Histidine Transporter 1.[60,79] However, L-histidine is a small water soluble molecule that can potentially permeate *in vitro* models to an extent via the paracellular pathway. Hence, the paracellular route cannot be ignored as it may contribute to a higher permeation rate of L-histidine in comparison to other transporter specific markers. Caffeine was also selected as a small hydrophilic psychostimulant that has been demonstrated to permeate the *in vivo* BBB, and we demonstrated its permeation across the direct contact triculture model.[80] Carbamazepine was selected as it is an anticonvulsant commonly used as a BBB positive marker and to our knowledge has not been shown to possess significant P-gp affinity.[81,82] In addition to R123, permeability of P-gp substrates colchicine and digoxin were assessed in the optimized model. The differences in permeation rates for separate P-gp substrates can be attributed to the broad substrate affinities and capacities of the efflux transporters and their relative expression levels. Further studies can be performed to assess the effect of P-gp inhibition on the permeation of these substrates as well as inhibition of other efflux transporters such as BCRP as there is also fairly significant substrate overlap across several efflux transporter isoforms. Clozapine is an antipsychotic that has been shown to be highly metabolized and may potentially inhibit P-gp.[69,83] Clozapine metabolites have also been demonstrated to have high BBB permeation, where additional studies using LC-mass spectrometry analysis and longer incubation time could be performed to elucidate the metabolic fate in the optimized triculture model.[83] Although, it is important to note that there were no metabolite peaks observed in the chromatograms during the time course of this study. Lastly, prazosin is a BCRP substrate that proved to have the lowest permeability of the selected markers. The low permeation of prazosin across the *in vitro* triculture model potentially suggests that functional BCRP activity is greater than that of P-gp or other efflux transporters, however further studies need to be performed to delineate the effects. The observed ranking of high and low BBB permeating compounds is ordered in a similar fashion to what has been seen by others both *in vitro* and *in vivo*.[84,85] The observed permeability of a small library of compounds across the optimized direct contact triculture model suggests that it is a useful tool for further assessment of BBB permeation of new chemical entities as well understanding of the synergistic effects of direct cell-cell contacts.

Conclusion

Herein, we have established an enhanced physiologically relevant *in vitro* model of the BBB by culturing the astrocytes, pericytes, and HBEC-5i cells in a layered, direct contact manner similar to the *in vivo* BBB that is comprised as part of the NVU. We provide

supporting evidence that apical cell layering removes the physical filter barrier observed in conventional triculture models and supports the potential of synergistic interactions occurring to provide a phenotype closer to the NVU. In addition, to our knowledge we are one of the first laboratories to utilize a three-stage multifactorial DOE based approach to expedite optimization of a BBB *in vitro* model. It is recommended that additional DOE based studies be performed to develop analogous models to mimic different pathologies of the brain, for example neurodevelopmental changes or neurodegenerative effects on the BBB with primary or proliferative cell lines.

The Blood Brain Barrier *in vitro* screening approaches have traditionally focused on tightening the brain microvessel endothelium that lines the capillaries, separates the blood from the neuronal environment, and maintains homeostasis. While screening models in the presence of astrocytes and pericytes in indirect contact to the BMECs have been developed, we postulated that direct contact of these cells, as found *in vivo*, would more adequately enhance *in vitro-in vivo* comparative studies. The direct layered culturing approach should enhance the synergistic effects by removing physical barriers and providing proximity so that secreted soluble factors and their effects on the regulation of the BMEC phenotype should be enhanced without added dilution and diffusion. Additionally, the ability for the model to rank established high and low brain permeating compounds alludes to its potential for BBB permeability screening of new chemical entities. This study also demonstrates the feasibility of using an informed DOE based approach to expedite culture development and can be further expanded for additional applications. Taken together, the direct contact triculture developed within appears to provide increased barrier properties that we theorize is attributable through facilitating adequate crosstalk between the three major cell types of the BBB that aids in the formation of the *in vivo* NVU. The findings of this work open the door for continued investigation of the roles of each BBB and potentially NVU cell type and its influence on barrier properties, as well as the establishment of a fully human, physiologically relevant *in vitro* model that can be used for moderate throughput screening to rank order potential neurotherapeutic compounds.

Funding

This work was supported in part by Environmental Protection Agency OSAPE Star Grant #RD-84002701-0.

Acknowledgments

The authors would like to acknowledge their co-inventors of US Patent No. 10877026 Dr. Christopher D. Kulczar, Dr. Monika Lavan, and Dr. Aimable Ngendahimana for their contributions to the establishment of this model.

Competing interest

Authors KL and GK are inventors under US Patent No. 10877026 which covers the work presented in this publication.

References

1. Pardridge WM. Why is the global CNS pharmaceutical market so under-penetrated? *Drug Discov Today*. 2002;7(1):5–7.
2. Gribkoff VK, Kaczmarek LK. The Need for New Approaches in CNS Drug Discovery: Why Drugs Have Failed, and What Can Be Done to Improve Outcomes. *Neuropharmacology*. 2017;120:11–19.
3. Kesselheim AS, Hwang TJ, Franklin JM. Two decades of new drug development for central nervous system disorders. *Nat Rev Drug Discov*. 2015;14(12):815–816.
4. Abbott NJ, Patabendige AAK, Dolman DEM, et al. Structure and function of the blood-brain barrier. *Neurobiol Dis*. 2010;37(1):13–25.
5. Abbott NJ. Blood-brain barrier structure and function and the challenges for CNS drug delivery. *J Inherit Metab Dis*. 2013;36(3):437–449.
6. Serlin Y, Shelef I, Knyazer B, et al. Anatomy and Physiology of the Blood-Brain Barrier. *Semin Cell Dev Biol*. 2015;38:2–6.
7. Weiss N, Miller F, Cazaubon S, et al. The blood-brain barrier in brain homeostasis and neurological diseases. *Biochim Biophys Acta*. 2009;1788(4):842–857.
8. Bauer HC, Krizbai IA, Bauer H, et al. 'You Shall Not Pass'-tight junctions of the blood brain barrier. *Front Neurosci*. 2014;8:392.
9. Haseloff RF, Dithmer S, Winkler L, et al. Transmembrane proteins of the tight junctions at the blood-brain barrier: structural and functional aspects. *Semin Cell Dev Biol*. 2015;38:16–25.
10. Wolburg H, Lippoldt A. Tight junctions of the blood-brain barrier: development, composition and regulation. *Vascul Pharmacol*. 2002;38(6):323–337.
11. Löscher W, Potschka H. Blood-brain barrier active efflux transporters: ATP-binding cassette gene family. *NeuroRx*. 2005;2(1):86–98.
12. Polli JW, Olson KL, Chism JP, et al. An Unexpected Synergist Role of P-Glycoprotein and Breast Cancer Resistance Protein on the Central Nervous System Penetration of the Tyrosine Kinase Inhibitor Lapatinib (N-{3-Chloro-4-[(3-fluorobenzyl)oxy]phenyl}-6-[5-({[2-(methylsulfonyl)ethyl]amino}methyl)-2-furyl]-4-quinazolinamine; GW572016). *Drug Metab Dispos*. 2009;37(2):439–442.
13. Abbott NJ, Rönnbäck L, Hansson E. Astrocyte-endothelial interactions at the blood-brain barrier. *Nat Rev Neurosci*. 2006;7(1):41–53.
14. Bouchaud C, Le Bert M, Dupouey P. Are close contacts between astrocytes and endothelial cells a prerequisite condition of a blood-brain barrier? The rat subfornical organ as an example. *Biol Cell*. 1989;67(2):159–165.
15. Bushong EA, Martone ME, Jones YZ, et al. Protoplasmic astrocytes in CA1 stratum radiatum occupy separate anatomical domains. *J Neurosci*. 2002;22(1):183–192.
16. Halassa MM, Fellin T, Takano H, et al. Synaptic islands defined by the territory of a single astrocyte. *J Neurosci*. 2007;27(24):6473–6477.
17. Wolburg H, Wolburg-Buchholz K, Fallier-Becker P, et al. Chapter one-Structure and Functions of Aquaporin-4-Based Orthogonal Arrays of Particles. *Int Rev Cell Mol Biol*. 2011;287:1–41.
18. Haseloff RF, Blasig IE, Bauer HC, et al. In search of the astrocytic factor(s) modulating blood-brain barrier functions in brain capillary endothelial cells in vitro. *Cell Mol Neurobiol*. 2005;25(1):25–39.
19. Lee SW, Kim WJ, Choi YK, et al. SSeCKS regulates angiogenesis and tight junction formation in blood-brain barrier. *Nat Med*. 2003;9(7):900–906.
20. Argaw AT, Gurfein BT, Zhang Y, et al. VEGF-mediated disruption of endothelial CLN-5 promotes blood-brain barrier breakdown. *Proc Natl Acad Sci U S A*. 2009;106(6):1977–1982.
21. Alvarez JI, Katayama T, Prat A. Glial influence on the Blood Brain Barrier. *Glia*. 2013;61(12):1939–1958.
22. Mathiisen TM, Lehre KP, Danbolt NC, et al. The perivascular astroglial sheath provides a complete covering of the brain microvessels: An electron microscopic 3D reconstruction. *Glia*. 2010;58(9):1094–1103.
23. Winkler EA, Bell RD, Zlokovic BV. Central nervous system pericytes in health and disease. *Nat Neurosci*. 2011;14(11):1398–1405.
24. Daneman R, Zhou L, Kebede AA, et al. Pericytes are required for blood-brain barrier integrity during embryogenesis. *Nature*. 2010;468(7323):562–566.

25. Gaengel K, Genové G, Armulik A, et al. Endothelial-mural cell signaling in vascular development and angiogenesis. *Arterioscler Thromb Vasc Biol*. 2009;29(5):630–638.

26. Hawkins BT, Davis TP. The Blood-Brain Barrier/Neurovascular Unit in Health and Disease. *Pharmacol Rev*. 2005;57(2):173–185.

27. Baeten KM, Akassoglou K. Extracellular Matrix and Matrix Receptors in Blood-Brain Barrier Formation and Stroke. *Dev Neurobiol*. 2011;71(11):1018–1039.

28. Weksler BB, Subileau EA, Perrière N, et al. Blood-brain barrier-specific properties of a human adult brain endothelial cell line. *FASEB J*. 2005;19(13):1872–1874.

29. Weksler B, Romero IA, Couraud PO. The hCMEC/D3 cell line as a model of the human blood brain barrier. *Fluids Barriers CNS*. 2013;10(1):16.

30. Helms HC, Abbott NJ, Burek M, et al. In vitro models of the blood-brain barrier: An overview of commonly used brain endothelial cell culture models and guidelines for their use. *J Cereb Blood Flow Metab*. 2016;36(5):862–890.

31. Tai LM, Reddy PS, Lopez-Ramirez MA, et al. Polarized P-glycoprotein expression by the immortalised human brain endothelial cell line, hCMEC/D3, restricts apical-to-basolateral permeability to rhodamine 123. *Brain Res*. 2009;1292:14–24.

32. Biemans EALM, Jäkel L, de Waal RMW, et al. Limitations of the hCMEC/D3 cell line as a model for Aβ clearance by the human blood-brain barrier. *J Neurosci Res*. 2017;95(7):1513–1522.

33. Urich E, Lazic SE, Molnos J, et al. Transcriptional profiling of human brain endothelial cells reveals key properties crucial for predictive in vitro blood-brain barrier models. *PloS One*. 2012;7(5):e38149.

34. Dorovini-Zis K, Prameya R, Bowman PD. Culture and characterization of microvascular endothelial cells derived from human brain. *Lab Investig*. 1991;64(3):425–436.

35. Wassmer SC, Combes V, Candal FJ, et al. Platelets Potentiate Brain Endothelial Alterations Induced by Plasmodium falciparum. *Infect Immun*. 2006;74(1):645–653.

36. Wassmer SC, Cianciolo GJ, Combes V, et al. Inhibition of Endothelial Activation: A New Way to Treat Cerebral Malaria? *PLoS Med*. 2005;2(9):e245.

37. Jambou R, Combes V, Jambou MJ, et al. Plasmodium falciparum adhesion on human brain microvascular endothelial cells involves transmigration-like cup formation and induces opening of intercellular junctions. *PLoS Pathog*. 2010;6(7):e1001021.

38. Jiang W, Huang W, Chen Y, et al. HIV-1 Transactivator Protein Induces ZO-1 and Neprilysin Dysfunction in Brain Endothelial Cells via the Ras Signaling Pathway. *Oxidative Medicine and Cellular Longevity*. 2017;2017:3160360.

39. Puech C, Hodin S, Forest V, et al. Assessment of HBEC-5i endothelial cell line cultivated in astrocyte conditioned medium as a human blood-brain barrier model for ABC drug transport studies. *Int J Pharm*. 2018;551(1-2):281–289.

40. Puech C, Delavenne X, He Z, et al. Direct oral anticoagulants are associated with limited damage of endothelial cells of the blood-brain barrier mediated by the thrombin/PAR-1 pathway. *Brain Res*. 2019:1719:57–63.

41. Dohgu S, Takata F, Yamauchi A, et al. Brain pericytes contribute to the induction and up-regulation of blood-brain barrier functions through transforming growth factor-beta production. *Brain Res*. 2005;1038(2):208–215.

42. Zozulya A, Weidenfeller C, Galla HJ. Pericyte-endothelial cell interaction increases MMP-9 secretion at the blood-brain barrier in vitro. *Brain Res*. 2008;1189:1–11.

43. Demeuse P, Kerkhofs A, Struys-Ponsar C, et al. Compartmentalized coculture of rat brain endothelial cells and astrocytes: a syngenic model to study the blood–brain barrier. *J Neurosci Methods*. 2002;121(1):21–31.

44. Thanabalasundaram G, El-Gindi J, Lischper M, et al. Methods to assess pericyte-endothelial cell interactions in a coculture model. *Methods Mol Biol*. 2011;686:379–399.

45. Li G, Simon MJ, Cancel LM, et al. Permeability of endothelial and astrocyte cocultures: in vitro blood-brain barrier models for drug delivery studies. *Ann Biomed Eng*. 2010;38(8):2499–2511.

46. Thomsen LB, Burkhart A, Moos T. A Triple Culture Model of the Blood-Brain Barrier Using Porcine Brain Endothelial cells, Astrocytes and Pericytes. *PloS One*. 2015;10(8):e0134765.

47. Wuest DM, Wing AM, Lee KH. Membrane configuration optimization for a murine in vitro blood–brain barrier model. *J Neurosci Methods*. 2013;212(2):211–221.

48. Hatherell K, Couraud PO, Romero IA, et al. Development of a three-dimensional, all-human in vitro model of the blood–brain barrier using mono-, co-, and tri-cultivation Transwell models. *J Neurosci Methods*. 2011;199(2):223–229.

49. McConnell HL, Kersch CN, Woltjer RL, et al. The Translational Significance of the Neurovascular Unit. *J Biol Chem*. 2017;292(3):762–770.

50. Malina KC-K, Cooper I, Teichberg VI. Closing the gap between the in-vivo and in-vitro blood–brain barrier tightness. *Brain Res*. 2009;1284:12–21.

51. Kulczar C, Lubin KE, Lefebvre S, et al. Development of a direct contact astrocyte-human cerebral microvessel endothelial cells blood-brain barrier coculture model. *J Pharm Pharmacol*. 2017;69(12):1684–1696.

52. Förster C, Burek M, Romero IA, et al. Differential effects of hydrocortisone and TNFα on tight junction proteins in an in vitro model of the human blood–brain barrier. J Physiol. 2008;586(7):1937–1949.

53. Paolinelli R, Corada M, Ferrarini L, et al. Wnt Activation of Immortalized Brain Endothelial Cells as a Tool for Generating a Standardized Model of the Blood Brain Barrier In Vitro. *PLoS One*. 2013;8(8):e70233.

54. Brown RC, Davis TP. Calcium modulation of adherens and tight junction function: a potential mechanism for blood-brain barrier disruption after stroke. *Stroke*. 2002;33(6):1706–1711.

55. De Bock M, Culot M, Wang N, et al. Low extracellular Ca2+ conditions induce an increase in brain endothelial permeability that involves intercellular Ca2+ waves. *Brain Res*. 2012;1487:78–87.

56. Hue CD, Cho FS, Cao S, et al. Dexamethasone potentiates in vitro blood-brain barrier recovery after primary blast injury by glucocorticoid receptor-mediated upregulation of ZO-1 tight junction protein. *J Cereb Blood Flow Metab*. 2015;35(7):1191–1198.

57. Lippmann ES, Al-Ahmad A, Azarin SM, et al. A retinoic acid-enhanced, multicellular human blood-brain barrier model derived from stem cell sources. *Sci Rep*. 2014;4:4160.

58. Mizee MR, Wooldrik D, Lakeman KAM, et al. Retinoic Acid Induces Blood–Brain Barrier Development. *J Neurosci*. 2013;33(4):1660–1671.

59. Ghandehari H, Smith PL, Ellens H, et al. Size-dependent permeability of hydrophilic probes across rabbit colonic epithelium. *J Pharmacol Exp Ther*. 1997;280(2):747–753.

60. Carl SM, Lindley DJ, Das D, et al. ABC and SLC transporter expression and proton oligopeptide transporter (POT) mediated permeation across the human blood-brain barrier cell line, hCMEC/D3 [corrected]. *Mol Pharm*. 2010;7(4):1057–1068.

61. Sorensen M, Steenberg B, Knipp GT, et al. The effect of beta-turn structure on the permeation of peptides across monolayers of bovine brain microvessel endothelial cells. *Pharm Res*. 1997;14(10):1341–1348.

62. Naik P, Cucullo L. In Vitro Blood–Brain Barrier Models: Current and Perspective Technologies. *J Pharm Sci*. 2012;101(4):1337–1354.

63. Bernas MJ, Cardoso FL, Daley SK, et al. Establishment of primary cultures of human brain microvascular endothelial cells to provide an in vitro cellular model of the blood-brain barrier. *Nat Protoc*. 2010;5(7):1265–1272.

64. Lacombe O, Videau O, Chevillon D, et al. In vitro primary human and animal cell-based blood-brain barrier models as a screening tool in drug discovery. *Mol Pharm*. 2011;8(3):651–663.

65. Knipp GT, Liu B, Audus KL, et al. Fatty acid transport regulatory proteins in the developing rat placenta and in trophoblast cell culture models. *Placenta*. 2000;21(4):367–375.

66. Gaston JD, Bischel LL, Fitzgerald LA, et al. Gene Expression Changes in Long-Term In Vitro Human Blood-Brain Barrier Models and Their Dependence on a Transwell Scaffold Material. *J Healthc Eng*. 2017;2017:5740975.

67. Lai CH, Kuo KH. The critical component to establish in vitro BBB model: Pericyte. *Brain Res Brain Res Rev*. 2005;50(2):258–265.

68. Armulik A, Genové G, Mäe M, et al. Pericytes regulate the blood-brain barrier. *Nature*. 2010;468(7323):557–561.

69. Maines LW, Antonetti DA, Wolpert EB, et al. Evaluation of the role of P-glycoprotein in the uptake of paroxetine, clozapine, phenytoin and carbamazapine by bovine retinal endothelial cells. *Neuropharmacology*. 2005;49(5):610–617.

70. Wedel-Parlow MV, Wölte P, Galla HJ. Regulation of major efflux transporters under inflammatory conditions at the blood-brain barrier in vitro. *J Neurochem*. 2009;111(1):111–118.

71. Eisenblätter T, Galla HJ. A new multidrug resistance protein at the blood-brain barrier. *Biochem Biophys Res Commun*. 2002;293(4):1273–1278.

72. Patching SG. Glucose Transporters at the Blood-Brain Barrier: Function, Regulation and Gateways for Drug Delivery. *Mol Neurobiol*. 2017;54(2):1046–1077.

73. Morgello S, Uson RR, Schwartz EJ, et al. The human blood-brain barrier glucose transporter (GLUT1) is a glucose transporter of gray matter astrocytes. *Glia*. 1995;14(1):43–54.

74. Xiuli G, Meiyu G, Guanhua D. Glucose Transporter 1, Distribution in the Brain and in Neural Disorders: Its Relationship With Transport of Neuroactive Drugs Through the Blood-Brain Barrier. *Biochem Genet*. 2005;43(3-4):175–187.

75. Amin Md L. P-glycoprotein Inhibition for Optimal Drug Delivery. Drug Target Insights. 2013;7:27–34.

76. Zhang L, Ong WY, Lee T. Induction of P-glycoprotein expression in astrocytes following intracerebroventricular kainate injections. *Exp Brain Res*. 1999;126(4):509–516.

77. Wang Q, Rager JD, Weinstein K, et al. Evaluation of the MDR-MDCK cell line as a permeability screen for the blood-brain barrier. *Int J Pharm*. 2005;288(2):349–359.

78. Hidalgo IJ. Assessing the absorption of new pharmaceuticals. *Curr Top Med Chem*. 2001;1(5):385–401.

79. Yamakami J, Sakurai E, Sakurada T, et al. Stereoselective blood-brain barrier transport of histidine in rats. *Brain Res*. 1998;812(1-2):105–112.

80. Chen X, Ghribi O, Geiger JD. Caffeine protects against disruptions of the blood-brain barrier in animal models of Alzheimer's and Parkinson's disease. *J Alzheimers Dis*. 2010;20(Suppl 1):S127–S141.

81. Grewal GK, Kukal S, Kanojia N, et al. In Vitro Assessment of the Effect of Antiepileptic Drugs on Expression and Function of ABC Transporters and Their Interactions with ABCC2. *Molecules*. 2017;22(10):1484.

82. Potschka H, Fedrowitz M, Löscher W. Brain access and anticonvulsant efficacy of carbamazepine, lamotrigine, and felbamate in ABCC2/MRP2-deficient TR- rats. *Epilepsia*. 2003;44(12):1479–1486.

83. Hellman K, Aadal Nielsen P, Ek F, et al. An ex Vivo Model for Evaluating Blood–Brain Barrier Permeability, Efflux, and Drug Metabolism. *ACS Chem Neurosci*. 2016;7(5):668–680.

84. Di Marco A, Gonzalez Paz O, Fini I, et al. Application of an in Vitro Blood-Brain Barrier Model in the Selection of Experimental Drug Candidates for the Treatment of Huntington's Disease. *Mol Pharm*. 2019;16(5):2069–2082.

85. Di Marco A, Vignone D, Gonzalez Paz O, et al. Establishment of an in Vitro Human Blood-Brain Barrier Model Derived from Induced Pluripotent Stem Cells and Comparison to a Porcine Cell-Based System. *Cells*. 2020;9(4):994.